

Absorption Spectra of Artificial Atoms in Presence of THz Fields

B. Dahiya, K.Batra, V.Prasad

Abstract—Artificial atoms are growing fields of interest due to their physical and optoelectronic applications. The absorption spectra of the proposed artificial atom in presence of Tera-Hertz field is investigated theoretically. We use the non-perturbative Floquet theory and finite difference method to study the electronic structure of Artificial Atom. The effect of static electric field on the energy levels of artificial atom is studied. The effect of orientation of static electric field on energy levels and dipole matrix elements is also highlighted.

Keywords—Absorption spectra, Artificial atom, Floquet Theory, THz fields

I. INTRODUCTION

WITH the development of technology advancements fabrication of artificial semiconductors is now possible [1,2]. Semiconductor nanostructures of different dimensions and shapes have been fabricated. Simultaneously many theoretical works have been developed to study such quantum confined structures [3],[4]. Out of those quantum confined structures, quantum dot have fascinated the scientific community due to their many physical and opto-electronic applications for example semiconductor lasers [5], quantum computing [6]-[8] and photodetectors [9],[10]. These structures have new electronic and optical properties depending upon the shape and size of the quantum dot and these properties help in improvement of various uses of electronic and optoelectronic devices [11]- [13]. As mentioned by U. Banin [14], due to their small size, more the transition between molecular and solid state regimes the quantum dots are described as ‘artificial atoms’ [15]-[17]. Quantum dots termed as artificial atoms, due to the similarities of their energy level structure, transition matrix elements can be used in many predominant effects such as quantum hall effect, quantum chaos [18]. There is an enhanced interest in the optical phenomenon based on the inter band and inter subband transitions in quantum dots, because of their potential applications [19]-[21] in the field of fundamental physics and chemistry. In this paper, we study the effect of static electric field on the absorption spectra of cubical quantum dot. We developed a model to study the electronic structure, dipole matrix elements and absorption spectra in electromagnetic field. The laser-‘artificial atom’ interaction is treated using non-perturbative Floquet method [4],[22],[23]. It is worth mentioning that we have studied the optical absorption spectra of a cubical quantum dot with finite confining potential.

B. Dahiya is with the Department of Physics, Swami Shradhanand College (University of Delhi) Delhi, India (+91-9968455498; e-mail: brijender.dahiya@gmail.com)

K. Batra is with University School of Basic and Applied sciences, GGS Indraprastha University, Delhi, India (e-mail: kriti.ipu@gmail.com).

V. Prasad is with the Department of Physics, Swami Shradhanand College (University of Delhi) Delhi, India (e-mail: vprasad@ss.du.ac.in).

Section II explains the theory behind the work, section III explains the computational method used here, section IV explains the results obtained and the last section V gives the concluding remarks about the work. To the best of our knowledge, it is the first study in the field.

II. THEORY

We have used the efficient and well tested non-perturbative Floquet theory that was originally developed to describe the atomic behavior in the presence of the intense laser fields proposed by Shirley [22], has been applied to numerous studies on atomic and molecular behavior in intense laser fields [4], [23]-[26]. We consider conduction band electron confined in a cubical quantum dot (CQD) having finite potential. This quantum dot is the ‘Artificial Atom’ having twenty seven bound levels. The quantum dot is subjected to static electric field E_s and a periodic perturbation in the term of a spatially homogeneous laser field \vec{E}_f . The laser field is applied in the ‘y’-direction and is given in the dipole approximation.

$$\vec{E}_f(t) = \hat{j}E_0 \cos(\omega t) \quad (1)$$

Where E_0 is the amplitude of the electric field, ω is the frequency of the laser field and \hat{j} is the polarization vector along ‘y’ direction. The time dependent Schrödinger equation for such a system is given by

$$H(t)\psi(t) = 0 \quad (2)$$

Where

$$H(t) = H_0 + erE_s + U(r, t) - \hat{i} \frac{\partial}{\partial t} \quad (3)$$

The Hamiltonian of the quantum system is periodic in time with period T such that $H(t + T) = H(t)$, where $\omega T = 2\pi$ and $\hbar = 1$. Here H_0 is the basis Hamiltonian, E_s is the static electric field strength and $U(r, t)$ is the interaction potential energy of the electron with the laser field. The wave function $\psi(t)$, called the quasi energy state (QES) or the Floquet state, can be written as

$$\psi(t) = \exp(-i\epsilon t)\phi(t) \quad (4)$$

Where ϵ is the real parameter, unique to multiplier of $2\pi n/T$, called the Floquet characteristic exponent or the quasi energy. The Floquet wave function $\phi(t)$ is also periodic in time with time period T . Expanding $\phi(t)$ and $H(t) = H_0 + erE_s + U(r, t)$, in terms of Floquet state basis gives

$$\begin{aligned} \Phi(t) &= \sum_{n=-\infty}^{+\infty} \phi_{\alpha\beta}^n e^{in\omega t} \\ H(t) &= \sum_{n=-\infty}^{+\infty} H_{\alpha\beta}^n e^{in\omega t} \end{aligned} \quad (5)$$

Where $\phi_{\alpha\beta}^n$ and $H_{\alpha\beta}^n$ are the Fourier amplitudes corresponding to a particular value of n (photon number). Substituting these expansions in the Schrödinger equation, one obtains an infinite set of recursion relations for $\phi_{\alpha\beta}^n$.

$$\sum_{\gamma k} [H_{\alpha\gamma}^{n-k} + n\omega\delta_{\alpha\gamma}\delta_{nk}] \Phi_{\gamma\beta}^k = \epsilon_\beta \Phi_{\alpha\beta}^n \quad (6)$$

The term in the bracket represents time independent Floquet Hamiltonian H_f . It follows from the equation (6) that the quasi energies are the eigenvalues of the Floquet equation.

$$\det[H_f \cdot \epsilon_\beta] = 0 \quad (7)$$

By diagonalising the Floquet matrix H_f , one can obtain the eigenvectors corresponding to eigenvalues ϵ_β . The absorption spectra probability for the excitation of the final state q from the initial state p summed over all the field states can be written as

$$P_{p \rightarrow q}^t = |\langle q | \hat{U}(t, t_0) | p \rangle|^2 \quad (8)$$

Where $U(t, t_0)$ is the evolution operator, however the quantity of experimental interest is the absorption spectra probability averaged over the initial time (t_0) keeping the elapsed time (t, t_0) fixed, is given by

$$P_{t \rightarrow t_0}^t = \sum_n \sum_{\epsilon_\beta} \left| \langle \Phi_{p\beta}^n | \exp(-i\epsilon_\beta(t - t_0)) | \Phi_{q\beta}^0 \rangle \right|^2 \quad (9)$$

Finally the continuous operation of the laser yields a long time averaged absorption spectra probability given by

$$P_{p \rightarrow q} = \lim_{T \rightarrow \infty} \left(\frac{1}{T} \right) \int_0^T P_{p \rightarrow q}^t(\tau) d\tau = \sum_n \sum_{\epsilon_\beta} |\Phi_{p\beta}^n \Phi_{q\beta}^0|^2 \quad (10)$$

III. COMPUTATION

We study the interaction of the laser field with a cubical quantum dot (i.e. Artificial Atom) in static electric field applied in 'y' direction. The potential function $V(r)$ or $V(x, y, z)$, required for the numerical solution, is the conduction band edge. The Eigen energies and the wavefunctions of the conduction band of CQD in static field are obtained by solving the time independent Schrödinger equation for the system, using finite difference method. This method has been implemented in various semiconductor heterostructures [27]-[29] to obtain the unperturbed eigenvalues and wavefunctions. This is a numerical method for solving the partial differential equation (PDE) based on discretization of the Hamiltonian on a spatial grid.

In the effective mass approximation, the Hamiltonian of an electron in conduction band in a cubical quantum dot in presence of static electric field E_s is [30]

$$H = H_0 + e\vec{E}_s \cdot \vec{r}$$

$$H = \frac{-\hbar^2}{2m^*} \nabla^2 + e\vec{E}_s \cdot \vec{r} + V(x, y, z) \quad (11)$$

With

$$V(x, y, z) = -228 \text{ meV} \quad |x|, |y|, |z| \leq \frac{L}{2} \\ = 0 \quad \text{elsewhere} \quad (12)$$

Where H_0 is the bare Hamiltonian, \vec{E}_s is the electric field vector, m^* and 'e' are the electron effective mass and charge respectively. \vec{r} is the position vector of the conduction band electron and L is the length of the dot. $V(x, y, z)$ or $V(r)$ is the finite confining potential.

The Schrödinger equation in presence of static electric field, under finite difference method can be written as follows:

$$H_0\psi + e r E_s \psi = - \frac{1}{2m_e^*} \left[\frac{\psi(r_{j+1}) - 2\psi(r_j) + \psi(r_{j-1}))}{\Delta^2} \right] \\ + V(r_j)\psi(r_j) + e r_j E_s \psi(r_j) \\ = E\psi \quad (13)$$

E is the energy eigen value in presence of static field, $\psi(r_j)$ is the eigenvector of the Schrödinger equation and $\Delta = r_{j+1} - r_j$ is the spacing between the two neighboring discrete points. In the limit $E_s \rightarrow 0$ the above equation gives the eigenvalues and wavefunctions for the unperturbed system.

The Hamiltonian ($H_0 + e r E_s$) is reduced to tridiagonal matrix and is diagonalised using standard Fortran subroutines to obtain the eigen values and the wave functions of a CQD. The Floquet theory is then implemented to obtain the Floquet Hamiltonian in the form of infinite matrix H_f . The Floquet Hamiltonian so obtained is shown below

$$H_f = \begin{pmatrix} \ddots & \ddots & \ddots & \ddots & \ddots & \ddots \\ \ddots & \ddots & \ddots & \ddots & \ddots & \ddots \\ \ddots & \ddots & \ddots & \ddots & \ddots & \ddots \\ \ddots & \ddots & \ddots & \ddots & \ddots & \ddots \\ \ddots & \ddots & \ddots & \ddots & \ddots & \ddots \\ 0 & B & 0 & 0 & 0 & 0 \\ B & A + 2I\omega & B & 0 & 0 & 0 \\ 0 & B & A + I\omega & B & 0 & 0 \\ 0 & 0 & B & A & B & 0 \\ 0 & 0 & 0 & B & A - I\omega & B \\ 0 & 0 & 0 & 0 & B & A - 2I\omega \\ \ddots & \ddots & \ddots & \ddots & \ddots & \ddots \end{pmatrix} \quad (14)$$

Where

$$A = \begin{pmatrix} 0 & 0 & 0 & 0 & 0 \\ 0 & E_1^s & 0 & 0 & 0 \\ 0 & 0 & E_2^s & 0 & 0 \\ 0 & 0 & 0 & E_3^s & 0 \\ 0 & 0 & 0 & 0 & E_4^s \end{pmatrix} \quad (15)$$

and

$$B = \begin{pmatrix} 0 & r_{12}^s & 0 & 0 \\ r_{21}^s & 0 & r_{23}^s & 0 \\ 0 & r_{32}^s & 0 & r_{34}^s \\ 0 & 0 & r_{43}^s & 0 \end{pmatrix} \quad (16)$$

The Floquet Hamiltonian matrix is an infinite dimensional matrix ($n = 0, \pm 1, \pm 2, \dots$) and possesses a block tridiagonal form. It has periodic structure with only number of ω varying in the diagonal elements from block to block. In the matrix H_f , E_n^s are the energy eigenvalues of the CQD in presence of static fields and $r_{mn}^s = -\frac{1}{2} E_0 \mu_{mn}^s$, where r_{mn}^s is off diagonal matrix and μ_{mn}^s denotes the dipole matrix element in presence of static electric fields. The optical behavior of the heterostructure is described by the oscillator strength of the transition between various energy levels of the quantum well defined as

$$f_{i \rightarrow j} = \frac{2m_0}{\hbar^2} (e_j - e_i) (Z_{ij})^2 \\ = \frac{2m_0}{\hbar^2} (e_j - e_i) (\mu_{ij})^2 \quad (17)$$

m_0 is the free electron mass (taken as $m_0 = 1$), e_i is the energy of i^{th} level and μ_{ij} is the dipole matrix element given by

$$\mu_{ij} = \int \psi_j^*(r) er \psi_i(r) dr \quad (18)$$

We obtain the quasi energies ϵ_β and corresponding Fourier components $\phi_{\alpha\beta}^n$ by diagonalising the Floquet Hamiltonian (14). The results converge after truncating H_f to only a few photon blocks.

IV. RESULTS AND DISCUSSION

In the present paper, we have investigated the variation of energy levels and dipole matrix elements of a cubical quantum dot acting as an artificial atom and also the transition probabilities of different levels is investigated for various values of static electric field value and the value of θ . Here θ is the angle between \vec{E}_s and the 'y-axis'. Dimension of the CQD acting as artificial atom is 10 \AA in each direction (i.e. $L_x = L_y = L_z = 10 \text{ \AA}$). Results shown here are in atomic units (otherwise mentioned). Considering various levels of the CQD as different levels of an artificial atom we can give nomenclature to the various levels depending upon the value of 'nlm' is given in Table 1. The value of 'n' gives the principal quantum number. From next two indices, the greater value defines the state (i.e. s, p or d) and the difference between them define the sublevel index (i.e. 0, ±1, ±2; also used in [3] and references therein). The notations used in one panel are same for all the corresponding panels.

TABLE I

TABLE INDICATES THE SYMBOLS AND THE NOTATIONS USED FOR THE DIFFERENT LEVELS OF THE ARTIFICIAL ATOM USED HERE

Sy mb ol	nlm	State	Sy mb ol	nlm	State	Sy mb ol	nlm	State
n1	111	1s ₀	n10	211	2s ₀	n19	311	3s ₀
n2	112	1p ₋₁	n11	212	2p ₋₁	n20	312	3p ₋₁
n4	121	1p ₊₁	n13	221	2p ₊₁	n22	321	3p ₊₁
n5	122	1p ₀	n14	222	2p ₀	n23	322	3p ₀
n3	113	1d ₋₂	n12	213	2d ₋₂	n21	313	3d ₋₂
n6	123	1d ₋₁	n15	223	2d ₋₁	n24	323	3d ₋₁
n8	132	1d ₊₁	n17	232	2d ₊₁	n26	332	3d ₊₁
n7	131	1d ₊₂	n16	231	2d ₊₂	n25	331	3d ₊₂
n9	133	1d ₀	n18	233	2d ₀	n27	333	3d ₀

The figure 1, explains the variation in the energy values of different levels as a function of static field strength. Each row has same value of θ and each column has same value of n. Value of θ in first row is 0° in middle row it is 10° and in last row it is 20° . The value of n is written on top of each column. It is clear from the figure that the different states shows the variation in their energy values with the increase in E_s but the variation decreases with increase in the value of θ . And the values are almost constant for $\theta = 20^\circ$. Some of the levels show the removal of degeneracy of the states.

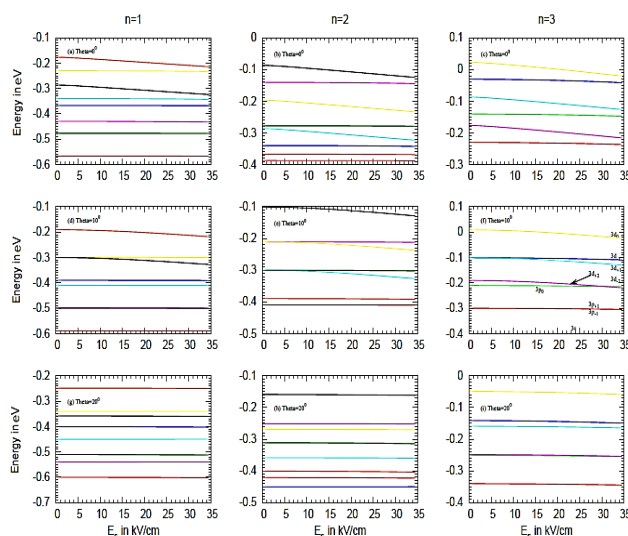


Fig. 1 The variation of energies of different levels is plotted as a function of Es. The value of n is indicated at the top of each column. And the value of $\theta = 0^\circ$ for 1st row, 10° for 2nd and 20° for the 3rd row. The notations shown in one of the panels is same for corresponding levels in other panels

In figure 2, we have shown the variation in absolute value of dipole matrix elements (|DME|) as a function of E_s for different values of θ . Here the DMEs shown are the dipole matrix elements between ground state and the corresponding states mentioned on each level. The DME shows the variation due to the change in energy and wavefunction of the corresponding states as we increase the value of the E_s . But apart from the strength of static electric field the orientation (θ) of the static electric field also plays an important role in the variation of DME, as shown in different panels of the figure. Thus for the variation in DME, the static field strength (E_s) and θ , both are effective.

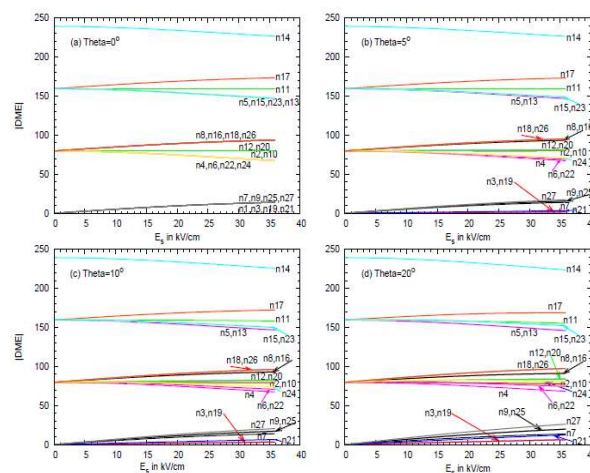


Fig. 2 The absolute values of dipole matrix elements (|DME|) between ground state (n1) and different states (n_j), with n_j indicated on each level, as a function of E_s for different values of θ is plotted. The value of θ is indicated in each panel

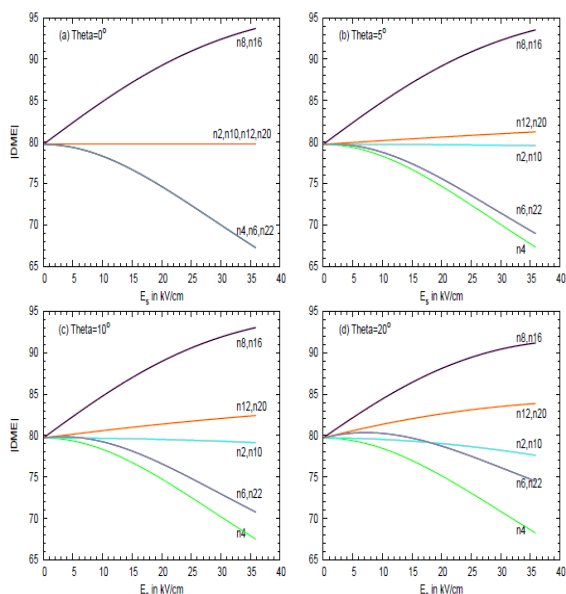


Fig. 3 The absolute values of dipole matrix elements ($|DME|$) between ground state (n_1) and some of the selected different states (n_j), with n_j indicated on each level, as a function of E_s for different values of θ is plotted. The value of θ is indicated in each panel

In figure 3, we have shown some selected levels from figure 2. In figure 3, it is quite clear how these levels show the variation in the values of $|DME|$ as a function of E_s . It is very clear from the figure that the variation in DME is due to the change in the energy and wave function of different levels with change in E_s and θ . It is also clear from the figure that the DMEs of these levels have same value at zero electric field and with the application of E_s and θ there is variation in DME. The figure 2 and 4(a) also explains that at $E_s=0$ there are only four possible values of DME between n_1 and n_j , where j varies from 1 to 27.

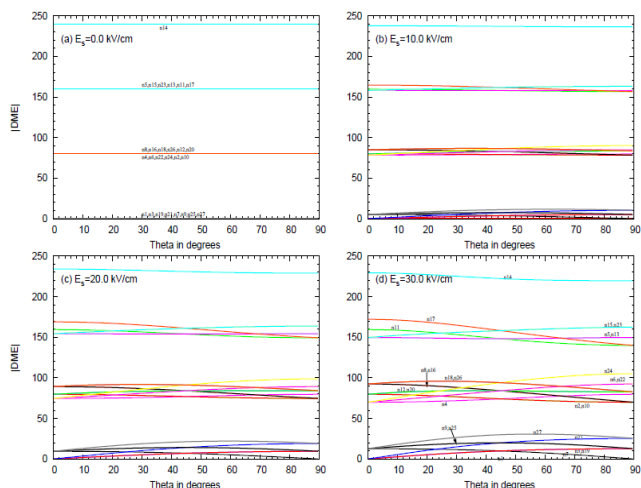


Fig. 4 The absolute values of dipole matrix elements ($|DME|$) between ground state (n_1) and different states (n_j), with n_j indicated on each level, as a function of θ for different values of E_s is plotted. The value of E_s is indicated in each panel. The notations shown in one of the panels is same for corresponding levels in other panels

In figure 4, the $|DME|$ between ground state (n_1) and different states (n_j), with n_j indicated on each level, are plotted as a function of θ for different values of E_s as indicated in each panel. The first panel shows that there are only four possible values of DME attained by all the levels. This can be compared with fig.2 at $E_s=0$ value. As the value of $E_s \neq 0$ the variation in DME of n_1 and corresponding n_j levels are obtained. The notations for different n_j are explained in panel (a) and panel (d). The notations in panel (d) are same for the corresponding DME values in rest of the panels. The variation in DME increases with increase in value of E_s .

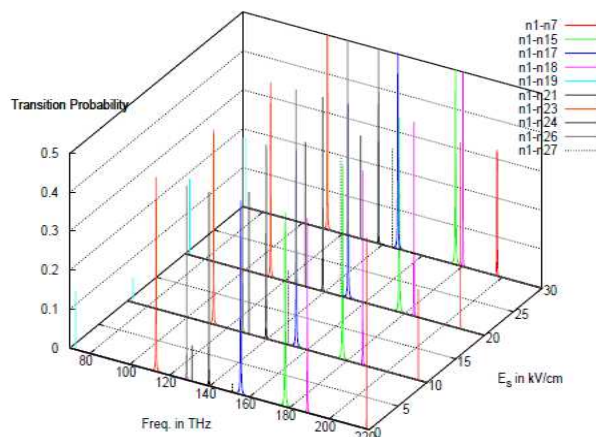


Fig. 5 The transition probabilities of some of the selected levels are shown as a function of laser frequency for different values of E_s , here $\theta = 10^0$ is kept constant

In figure 5, the transition probabilities of some of the selected levels are shown as a function of laser frequency. The different plots are for various values of E_s at $\theta = 10^0$. It is clear from the figure that there is red-shifting of some levels with increase in the value of E_s . Also the value of transition probability alters for different values of E_s .

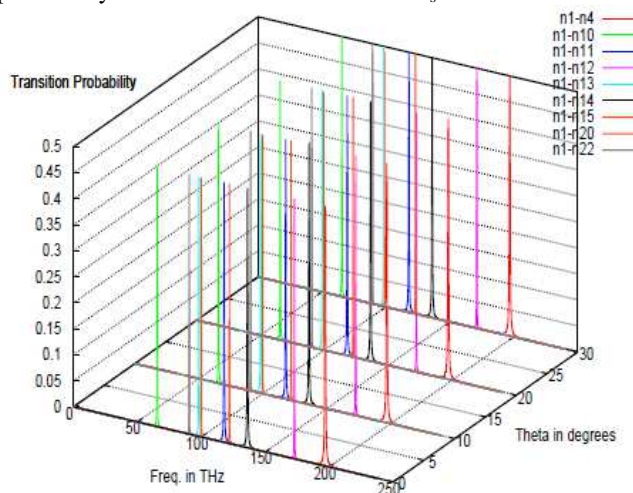


Fig. 6 The transition probabilities of some of the selected levels are shown as a function of laser frequency for different values of θ , here $E_s = 20$ kV/cm is kept constant

In figure 6, the transition probabilities of some of the selected levels are shown as a function of laser frequency. The different plots are for various values of θ at $E_s = 20$ kV/cm. In this figure, it is clear that for various values of θ , we do not get any red-shifting but the values of transition probabilities shows some variations for different values of θ .

V. CONCLUSION

The various properties of the artificial atom are studied. The degeneracy of the levels of artificial atom is removed when the external static electric field is applied along one of the directions (here y-direction). Due to the removal of the degeneracy new absorption peaks are observed in the absorption spectra of the artificial atom. This may give rise to various other features such as linear and non-linear absorption coefficients and refractive index changes of the material of which the atom is made of. (Work in this regard is in progress and will be published soon).

REFERENCES

[1] T. Raz, D. Ritter, and G. Bahir, "Formation of InAs self-assembled quantum rings on InP," *Appl. Phys. Lett.*, vol. 82, pp. 1706-1708, March 2003

[2] D. Granados and J. M. Garcia, "In(Ga)As self-assembled quantum ring formation by molecular beam epitaxy," *Appl. Phys. Lett.*, vol. 82, pp. 2401-2403, April 2003

[3] V. Prasad and P. Silotia, "Effect of laser radiation on optical properties of disk shaped quantum dot in magnetic fields," *Phys. Lett. A*, vol. 375, pp. 3910-3915, October 2011

[4] V. Prasad and B. Dahiya, "Modifications of laser field assisted intersubband transitions in the coupled quantum wells due to static electric field," *Physica Status Solidi B*, vol. 248, pp. 1727-1734, July 2011

[5] N. Kirstaedter, O. G. Schmidt, N. N. Ledentsov, D. Bimberg, V. M. Ustinov, A. Yu. Egorov, A. E. Zhukov, M. V. Maximov, P. S. Kopev, and Zh. I. Alferov, "Gain and differential gain of single layer InAs/GaAs quantum dot injection lasers," *Appl. Phys. Lett.*, vol. 69, pp. 1226-1228, August 1996

[6] D. Bimberg, "Quantum dots for lasers, amplifiers and computing," *J. Phys. D*, vol. 38, pp. 2055-2058, July 2005 and references therein

[7] D. Loss and D.P. DiVincenzo, "Quantum computation with quantum dots," *Phys. Rev. A*, vol. 57, pp. 120-126, January 1998 and references therein

[8] K. R. Brown, D. A. Lidar, and K. B. Whaley, "Quantum computing with quantum dots on quantum linear supports," *Phys. Rev. A*, vol. 65, pp. 012307[19 pages], December 2001

[9] S. Maimon, E. Finkman, G. Bahir, S. E. Schacham, J. M. Garcia, and P. M. Petroff, "Intersublevel transitions in InAs/GaAs quantum dots infrared photodetectors," *Appl. Phys. Lett.*, vol. 73, pp. 2003-2005, October 1998

[10] Eui-Tae Kim, A. Madhukar, Z. Ye and J. C. Campbell, "High detectivity InAs quantum dot infrared photodetectors," *Appl. Phys. Lett.*, vol. 84, pp. 3277-3279, April 2004

[11] D. Ahn and S.L. Chuang, "Calculation of linear and nonlinear intersubband optical absorptions in a quantum well model with an applied electric field," *IEEE J. Quantum Electron.*, vol. QE-23, pp. 2196-2204, December 1987

[12] X. Zhang, G. Xiong and X. Feng, "Well width-dependent third-order optical nonlinearities of a ZnS/CdSe cylindrical quantum dot quantum well," *Physica E*, vol. 33, pp. 120-124, June 2006

[13] I. Karabulut, S. Unlu and H. Safak, "Calculation of the changes in the absorption and refractive index for intersubband optical transitions in a quantum box," *Physica Status Solidi B*, vol. 242, pp. 2902-2909, November 2005

[14] U. Banin, Y.W. Cao, D. Katz and O. Millo, "Identification of atomic-like electronic states in indium arsenide nanocrystal quantum dots," *Nature*, vol. 400, pp.542-544, August 1999

[15] A. P. Alivisatos, "Semiconductor Clusters, Nanocrystals, and Quantum Dots," *Science*, vol. 271, pp. 933-937, February 1996

[16] M. A. Kastner, "Artificial Atoms," *Phys. Today*, vol. 46(1), pp. 24-31, January 1993

[17] R.C. Ashoori, "Electrons in artificial atoms," *Nature*, vol. 379, pp. 413-419, February 1996

[18] A.D. Stone and H. Bruus, "Chaos and fluctuations in quantum dots," *Physica B*, vol. 189, pp. 43-56, June 1993

[19] J. L. Liu, Y. S. Tang, K. L. Wang, T. Radetic, and R. Gronsky, "Raman scattering from a self-organized Ge dot superlattice," *Appl. Phys. Lett.*, vol. 74, pp. 1863-1865, March 1999

[20] J. L. Liu, W. G. Wu, A. Balandin, G. L. Jin, and K. L. Wang, "Intersubband absorption in boron-doped multiple Ge quantum dots," *Appl. Phys. Lett.*, vol. 74, pp. 185-187, January 1999

[21] S. Abdi-Ben Nasrallah, A. Bouazra, A. Poncet, and M. Said, "Theoretical investigation of intersubband transition energies and oscillator strength in CdS/SiO₂ quantum dots," *Physica E*, vol. 43, pp. 146-150, November 2010

[22] J. H. Shirley, "Solution of the Schrödinger Equation with a Hamiltonian Periodic in Time," *Phys. Rev.*, vol. 138, pp. B979-B987, May 1965

[23] Shih-I Chu, "Recent Developments in Semiclassical Floquet Theories for Intense-Field Multiphoton Processes," *Adv. At. Mol. Phys.*, vol. 21, pp. 197-253, July 1985

[24] M. Mohan and V. Prasad, "Laser-assisted vibrational excitations during ion-molecule collisions," *J. Phys. B*, vol. 24, pp. L81-L87, February 1991

[25] V. Prasad, B. Sharma and M. Mohan, "Excitation of atomic hydrogen due to proton impact in the presence of a resonant laser field," *Physica Scripta*, vol. 52, pp. 372-376, April 1995

[26] U. Arya, B. Dahiya and V. Prasad, "l-Mixing Collision in Presence of Microwave Field," *J. Mod. Phys.*, vol. 3, pp. 28-36, January 2012

[27] T. B. Boykin and G. Klimeck, "The discretized Schrödinger equation and simple models for semiconductor quantum wells," *Eur. J. Phys.*, vol. 25, pp. 503-514, July 2004

[28] W. H. Ng and K. S. Chan, "An analytical expression for quantum-well tunneling lifetimes," *J. Appl. Phys.*, vol. 93, pp. 2630-2637, March 2003

[29] M. Gudwani, V. Prasad, P. K. Jha, and M. Mohan, "Intersubband Transitions in Coupled Quantum wells under an intense Laser Field," *Int. J. Nanosci.*, vol. 7, pp. 215-221, August 2008

[30] Zhi-Hai Zhang, Kang-Xian Guo, Bin Chen, Rui-Zhen Wang, Min-Wu Kang, "Third-harmonic generation in cubical quantum dots," *Superlattices and Microstructures*, vol. 46, pp. 672-678, October 2009